Received: 8 July 2023 | Revised: 23 October 2023 | Accepted: 30 November 2023

DOI: 10.1111/sapm.12663

STUDIES IN APPLIED MATHEMATICS WILEY

ORIGINAL ARTICLE

Dynamics of 2D fluid in bounded domain via conformal variables

Alexander Chernyavsky | **Sergey Dyachenko**

Department of Mathematics, State University of New York at Buffalo, Buffalo, New York, USA

Correspondence
Alexander Chernyavsky, Department of Mathematics, State University of New York at Buffalo, Buffalo, New York 14260, USA.
Email: chernyav@buffalo.edu

Abstract

In the present work, we compute numerical solutions of an integro-differential equation for traveling waves on the boundary of a 2D blob of an ideal fluid in the presence of surface tension. We find that solutions with multiple lobes tend to approach Crapper capillary waves in the limit of many lobes. Solutions with a few lobes become elongated as they become more nonlinear. It is unclear whether there is a limiting solution for small number of lobes, and what are its properties. Solutions are found from solving a nonlinear pseudodifferential equation by means of the Newton conjugate-residual method. We use Fourier basis to approximate the solution with the number of Fourier modes up to $N = 65536$.

KEYWORDS
bounded domain, conformal mapping, water waves

1 | INTRODUCTION

The capillary waves are commonly observed in the ocean swell on the length scale of a few centimeters. They often appear as a result of breaking of steep gravity waves[1] or other processes related to water wave turbulence, such as the formation of direct energy cascade.[2,3] When wind blows on the ocean surface, or a breaking ocean wave is observed, a spray of droplets often is formed when tiny droplets detach from the main body of water.

Leaving aside the ballistic motion induced by gravity, the internal motion of a droplet is dominated by the kinetic energy entrapped in its body, and the surface tension forces acting upon its

free surface. The perfect sphere is a minimizer of the surface area of a fluid droplet, and hence, potential energy due to surface tension attains its minimum value in a spherical droplet. Similarly, in a 2D fluid, the minimal perimeter is attained by a disc-shaped droplet. Once detached from the bulk of the fluid, it carries away angular momentum from the fluid body as a part of its kinetic energy. Both quantities are conserved in time and contribute to its dynamics that can be quite complicated, and is described by the Euler equations with a free boundary. When the angular momentum carried by a droplet is too large to be balanced by surface tension, the droplet may break further into even smaller droplets, and a cascade of multiple breaking droplets observed on a large scale may be contributing to generation of water spray at the crests of steep ocean waves. Some environmental processes, like the gas exchange at the air–water interface, can be greatly enhanced by an effective increase of surface area through droplet generation. It is our aim to understand the internal dynamics of droplets, and the processes that may result in their breaking.

In the present work, we consider nonlinear traveling waves on the free surface of a droplet of radius R induced by a balance of angular momentum and the forces of surface tension. We follow the conformal variables approach originally introduced by Stokes in Ref. [4] and later extended to time-dependent problem in Refs. [5, 6]. A framework for studying flows in closed domains (like a fluid blob) as well as on the exterior of an air bubble submerged in a 2D ideal fluid has been developed in Ref. [7] focusing on fluid flows generated by point vortex. In contrast to Ref. [7], we make no additional assumption on the nature of the velocity field. Our approach is based on the conformal variables technique for bounded domains described in Ref. [8].

We find families of nonlinear traveling waves that bifurcate from a disc-shaped droplet and can be parameterized by an integer number of wavelengths per perimeter of a droplet (the number of lobes, k) and the wave steepness. The solutions are found numerically in terms of Fourier series satisfying pseudodifferential nonlinear eigenvalue problem that is qualitatively similar to the Babenko equation for Stokes waves in 2D[9] and can be solved by similar numerical techniques.[10,11]

Given wave length λ, we recover the family of Crapper wave solutions[12,13] in the limit $\lambda \ll R$ ($k \to \infty$). This limit is equivalent to traveling capillary waves in infinite depth fluid. Oscillations of 3D droplets have been a subject of interest since the works of Rayleigh,[14] and have been studied both experimentally and analytically, see, for example, Ref. [15]. It is yet unclear whether there is a relation between dynamics of 2D and 3D droplets.

The text is organized as follows. In the first three sections, we describe the motion integrals relevant to droplet mechanics, the conformal variables approach, and the equation (10) describing a nonlinear traveling wave. Section 4 describes the series solution for infinitesimal waves that are employed as the initial guess in the Newton conjugate-residual (CR) method[10,11] in Section 5. The main results and conclusions are described in Section 7.

2 | PROBLEM FORMULATION

We consider the motion of a 2D ideal fluid in a bounded domain $\mathcal{D}$. The velocity field is given by the gradient of the velocity potential, $\varphi(\mathbf{r}, t)$, where $\mathbf{r} = (x, y)^T \in \mathcal{D}$.

The Hamiltonian is the sum of kinetic and potential energy due to the surface tension:

$$\mathcal{H} = \frac{1}{2} \iint_{\mathcal{D}} (\nabla\varphi)^2 \, dxdy + \sigma \int_{\partial\mathcal{D}} dl, \tag{1}$$

where ∇ is the 2D gradient and σ is the surface tension coefficient. The boundary of the fluid domain, ∂D, also known as the free surface, is a time-dependent curve in 2D.

When the fluid is at rest, the shape of the droplet is a perfect disc, a shape that attains the least perimeter given a fixed volume μ; when detached from the body of fluid, droplet carries away angular momentum $\mathcal{J}$ that is conserved:

$$\mu = \iint\limits_D dxdy \quad \text{and} \quad \mathcal{J} = \iint\limits_D [\mathbf{r} \times \nabla\varphi]\, dxdy. \tag{2}$$

A semi-infinite periodic strip $w = u + iv \in \{-\pi \le u < \pi, v \le 0\}$ is conformally mapped to the fluid domain $z = x + iy \in D$ by the complex function $z(w, t)$. The invariant quantities associated with the flow may be expressed in terms of conformal variables as $1D$ integrals over the free surface $w = u$ ($v = 0$); for example, the Hamiltonian becomes

$$\mathcal{H} = \frac{1}{2}\iint\limits_D (\nabla\varphi)^2\, dxdy + \sigma\int\limits_{\partial D} dl = \frac{1}{2}\int\limits_{-\pi}^{\pi} \psi\hat{k}\psi\, du + \sigma\int\limits_{-\pi}^{\pi} |z_u|\, du, \tag{3}$$

where $\hat{H}$ is the Hilbert transform, and $\hat{k} = -\hat{H}\partial_u$. Here, $\psi(u, t) = \varphi(x(u, t), y(u, t), t)$ is the velocity potential at the free surface. The total volume of an incompressible fluid is proportional to the mass of the fluid μ, a trivial constant of motion, and the angular momentum $\mathcal{J}$, given by

$$\mu = \iint\limits_D dx\, dy = \frac{1}{4i}\int\limits_{-\pi}^{\pi} [z\bar{z}_u - \bar{z}z_u]\, du, \tag{4}$$

$$\mathcal{J} = \iint\limits_D [\mathbf{r} \times \nabla\phi]\, dxdy = -\frac{1}{2}\int\limits_{\partial D} r^2\frac{\partial\theta}{\partial\mathbf{n}}\, dl = -\frac{1}{2}\int\limits_{-\pi}^{\pi} |z|^2\psi_u\, du, \quad \frac{d\mathcal{J}}{dt} = 0, \tag{5}$$

where $r = \sqrt{x^2 + y^2}$ and $\mathbf{n}$ is the unit normal to the free surface.

3 | TRAVELING WAVE

The implicit form of complex equations of motion is given by:

$$z_t\bar{z}_u - \bar{z}_t z_u = \bar{\Phi}_u - \Phi_u, \tag{6}$$

$$\psi_t\bar{z}_u - \psi_u\bar{z}_t + \frac{\Phi_u^2}{2z_u} = i\sigma\partial_u\left(\frac{\bar{z}_u}{|z_u|}\right), \tag{7}$$

where $\Phi = \psi + i\hat{H}\psi =: 2\hat{P}\psi$ is the complex potential and we defined the projection operator, $\hat{P} = \frac{1}{2}(1 + i\hat{H})$.

A traveling wave on the free surface of a disc is obtained by seeking conformal map and potential in the form:

$$z(u,t) = e^{-i\Omega t} z(u - \Omega t) \quad \text{and} \quad \Phi(u,t) = i\Omega \hat{P}|z|^2 - \beta t, \tag{8}$$

where β is the Bernoulli constant. We note that the equations of motion are invariant under the change of variables $u \to u - \Omega t$, and thus, the solution may be sought in the form $z = z(u)$. Substitution of (8) in the equations (6) and (7) leads to an equation for traveling waves:

$$2\beta y_u - \frac{\Omega^2}{2}\left[x\hat{k}|z|^2 - \hat{H}\left(y\hat{k}|z|^2\right)\right] - \sigma\partial_u\left[\frac{x_u}{|z_u|} - \hat{H}\left(\frac{y_u}{|z_u|}\right)\right] = 0, \tag{9}$$

or, in the complex form,

$$2i\beta z_u + \Omega^2 \hat{P}\left[z\hat{k}|z|^2\right] + 2\sigma\partial_u \hat{P}\left[\frac{z_u}{|z_u|}\right] = 0. \tag{10}$$

For a traveling wave solution, kinematic constants are related via the formula

$$\mu\beta = \Omega\mathcal{J} + \frac{\sigma}{2}L, \tag{11}$$

where

$$L = \int_{-\pi}^{\pi} |z_u| du \tag{12}$$

is the perimeter of the droplet.

4 | ASYMPTOTIC SERIES FOR SMALL WAVES

Let $w = u + iv \in \mathbb{C}^-$, and recall that e^{-iw} is a conformal map from a semi-infinite strip $-\pi < u < \pi$ and $v < 0$ to a unit disc. The function $z(u)$ describing the shape of a small amplitude wave is represented by an infinite Fourier series,

$$z(u) = e^{-iu}\left(1 + \sum_{k=1}^{\infty} a_k e^{-iku}\right), \tag{13}$$

where a_k are the Fourier coefficients. Unless the solution is strongly nonlinear, the series is rapidly convergent, and asymptotic solution of the Equation (10) can be obtained by a series expansion (13) assuming $|a_2| \ll |a_1|$.

The first-order approximation is given by

$$z = e^{-iu}\left(1 + a_k e^{-iku}\right), \tag{14}$$

where $k \geq 2$ is an integer representing the number of lobes in the solution. When ansatz (14) is plugged into the dynamic condition (7), we find that the Bernoulli constant, β, and frequency, Ω,

must be expanded in series keeping $O(a_k)$ terms as follows;

$$\beta = \sigma + O(a_k^2), \quad \Omega^2 = \frac{(k^2-1)\sigma}{k} + O(a_k^2). \tag{15}$$

Dispersion is the relation between frequency of rotation, $\Omega(k)$, and wave number. As shown in Ref. [8], it can be obtained from (7) via asymptotic expansion in a_k. The nonlinear dispersion relation is obtained numerically.

The second-order approximation to the solutions of (10) can be found by keeping the first two terms in the Fourier expansion (13). We will consider the case of $k = 2$, but generalization to arbitrary number of lobes k can be done analogously. We now seek solution in the form:

$$z = e^{-iu}\left(1 + a_2 e^{-2iu} + a_4 e^{-4iu}\right), \tag{16}$$

and substitute it into Equation (10) for traveling waves to match the corresponding terms in the expansion. We expand Equation (10) in Fourier series and require that the first three series' coefficients vanish, which results in the following expressions:

$$\begin{aligned}
&e^{-iu}\left[2(\beta-\sigma) + \frac{1}{128}\left(64(9\sigma+4\Omega^2)a_2^2\right) + O(a_2^4)\right] && \text{(determines } \beta\text{)}\\
&+ e^{-3iu}a_2\left[(6\beta - 9\sigma + 2\Omega^2) + \left(\frac{9}{8}(-9a_2^2 + 20a_4)\sigma + 4a_4\Omega^2\right) + O(a_2^4)\right] && \text{(determines } \Omega^2\text{)}\\
&+ e^{-5iu}\left[128\left(5(8a_4\beta + 9a_2^2\sigma - 20a_4\sigma) + 8(a_2^2 + 2a_4)\Omega^2\right) + O(a_2^4)\right], && \text{(determines } a_4\text{)}
\end{aligned}$$

thus the second-order approximation for the Bernoulli constant β and frequency Ω are determined by

$$\beta = \sigma\left(1 - \frac{15}{4}a_2^2\right) + O(a_2^4), \quad \Omega^2 = \sigma\left(\frac{3}{2} - \frac{25}{4}a_2^2\right) + O(a_2^4),$$

and $a_4 = \frac{19}{12}a_2^2$. The first- and second-order approximations are used to provide the initial guess for the Newton's method applied to the fully nonlinear equation (10). The discussion of fully nonlinear solutions and implementation of Newton's method is presented in the following sections.

In a more general case, $k \geq 2$, the second-order approximation is found analogously:

$$z = e^{-iu}(1 + a_k e^{-iku} + a_{2k} e^{-2iku}) + O(a_k^3), \tag{17}$$

and by repeating the same steps to keep orders up to $O(a_k^2)$, we obtain

$$\beta = \left(1 - \frac{a_k^2}{4}(k+1)(3k-1)\right)\sigma + O(a_k^4), \tag{18a}$$

$$\Omega^2 = \frac{k^2-1}{4k(1+2k^2)}\left(4 + 8k^2 + a_k^2(1+k)(6 - k(22 + k + k^2))\right)\sigma + O(a_k^4), \tag{18b}$$

$$a_{2k} = \frac{(1+k)((7+2k)k-3)}{4(1+2k^2)}a_k^2 + O(a_k^4). \tag{18c}$$

Conformal map (17) with parameters (18) can serve as an initial guess for numerical iterative procedure such as Newton's method.

5 | NEWTON'S METHOD

The nonlinear solutions of (10) are found by applying Newton's iterations. Given an initial guess, $z^{(0)}(u)$, or an approximation, $z^{(m)}$ at an iteration m, we may write the exact solution of (10) as follows:

$$z = z^{(m)} + \delta z, \tag{19}$$

where z is the unknown exact solution of (10), $m \geq 0$ is the iteration number, and δz is the correction term to be determined. The formula (19) is substituted into Equation (10) assuming $||\delta z|| \ll ||z^{(m)}||$ and only the linear terms in δz are kept:

$$2i\beta\delta z_u + \Omega^2\hat{P}\left[\delta z\hat{k}\left|z^{(m)}\right|^2 + z^{(m)}\hat{k}\left(z^{(m)}\delta\bar{z} + \bar{z}^{(m)}\delta z\right)\right]$$

$$+\sigma\partial_u\hat{P}\left[\frac{z_u^{(m)}}{\left|z_u^{(m)}\right|^3}\left(\bar{z}_u^{(m)}\delta z_u - z_u^{(m)}\delta\bar{z}_u\right)\right] + \hat{N}(z^{(m)}) = 0,$$

where $N(z)$ is defined as follows:

$$\hat{N}(z) := 2i\beta z_u + \Omega^2\hat{P}\left[z\hat{k}|z|^2\right] + 2\sigma\partial_u\hat{P}\left[\frac{z_u}{|z_u|}\right], \tag{20}$$

which is exactly the left-hand side of Equation (10). It is often more convenient to implement iterations for a real unknown function, and we may recall that the components of the conformal map are not independent and are related via the Hilbert transform, that is, since $z = x + iy$ and $\delta z = \delta x + i\delta y$, then

$$x = -\hat{H}y, \quad \delta x = -\hat{H}[\delta y],$$

and the linearized equation (20) is equivalent to an auxiliary real equation for one real unknown function δy given by

$$L_1(y)\delta y + L_0(y) = 0, \tag{21}$$

where we have defined the operators L_0 and its linearization $L_1(y)$ as follows:

$$L_0(y) := -2\beta y_u + \frac{1}{2}\Omega^2\left(x\hat{k}|z|^2 - \hat{H}\left[y\hat{k}|z|^2\right]\right) + \sigma\partial_u\left(\frac{x_u}{|z_u|} - \hat{H}\left[\frac{y_u}{|z_u|}\right]\right), \tag{22}$$

$$L_1(y)\delta y := -2\beta\delta y_u + \frac{\Omega^2}{2}\left(\delta x\hat{k}|z|^2 + x\hat{k}(x\delta x + y\delta y) - \hat{H}\left[\delta y\hat{k}|z|^2 + y\hat{k}(x\delta x + y\delta y)\right]\right) \tag{23}$$

$$+\sigma\partial_u\left(-\frac{y_u}{|z_u|^3}(x_u\delta y_u - y_u\delta x_u) + \hat{H}\left[\frac{x_u}{|z_u|^3}(x_u\delta y_u - y_u\delta x_u)\right]\right). \tag{24}$$

When Hilbert transform is applied to Equation (21), we obtain the linear equation for δy:

$$\hat{H}L_1\delta y = -\hat{H}L_0 \tag{25}$$

with an operator, HL_1, which is self-adjoint with respect to the standard inner product:

$$(f,g) = \int_{-\pi}^{\pi} f(x)g(x)dx \tag{26}$$

for real-valued $f(x)$ and $g(x)$. The resulting linear system is solved by means of the CR method. We solve (21) numerically using a Fourier pseudospectral method to approximate the function δy. The projection operator $\hat{P}$, Hilbert transform $\hat{H}$, and differentiation with respect to u are applied as Fourier multipliers. At each Newton iteration, a new linear system is solved with CR. Newton's iterations are performed until a required tolerance, ε, is attained: $\|\hat{N}(z^{(m)})\| \le \varepsilon$.

The second-order approximation (17) is used as an initial guess, $z^{(0)}$, to initiate the Newton's iterations. Once a nonlinear solution is determined with a given set of parameters, it is used to follow the solution branch to strongly nonlinear waves by parameter continuation, either in β or Ω^2, while keeping surface tension σ fixed.

The constraint (11) relating the physically relevant quantities μ (see (4)), $\mathcal{J}$ (see (5)), and L (see (12)) is used to determine the value of Ω^2 if β is known, or vice versa:

$$-i\beta\int_{-\pi}^{\pi} z\overline{z}_u - \overline{z}z_u du + 2\Omega^2\int_{-\pi}^{\pi}|z|^2\hat{k}|z|^2 du - 2\sigma\int_{-\pi}^{\pi}|z_u|du = 0. \tag{27}$$

The solutions of (10) enjoy two symmetries, one is related to the freedom of choosing the phase shift in the rotation angle, and the second symmetry is related to rescaling of the droplet surface. The choice of phase shift is fixed by seeking only even $y(u)$, and in order to hold the droplet area μ fixed, we rescale $z(u)$, β, L, and $\mathcal{J}$ once a solution of (10) is obtained,

$$z(u) \to \frac{z}{\nu}, \quad \mu \to \frac{\mu}{\nu^2}, \quad L \to \frac{L}{\nu}, \quad \mathcal{J} \to \frac{\mathcal{J}}{\nu^4}. \tag{28}$$

For example, choosing $\nu = \sqrt{\mu/\pi}$ ensures that $\mu = \pi$ is preserved. The number of Fourier modes that we considered is limited by $N = 65536$, and the magnitude of the Fourier mode at series truncation is 10^{-9}. The relative tolerance for solving the linear system (21) in the CR method is 10^{-2}, and the nonlinear residual for Newton's iterations $\varepsilon = 10^{-9}$.

A higher number of modes (up to $N = 65536$) is required because even though the solution profiles may appear smooth, the distribution of points is not equal. There is a scarcity of points near the edges of the lobes, whereas the number of points is dense in between the lobes. To achieve a more accurate Fourier approximation, one could consider using auxiliary coordinate transformation.[16]

6 | MAIN RESULTS

The nonlinear waves obtained with Newton CR method are illustrated in Figure 1 with $k = 4$ and $k = 25$ lobes. In addition, we show parameter curves Ω^2 versus H/λ (see Figure 2, left) and $\mathcal{J}$ versus H/λ (see Figure 2, right). Here, H denotes the height of the wave, and λ is the spatial period.

We illustrate two typical solutions of the nonlinear equation (10) by showing the shape of the free surface and the velocity field in Figure 3. We find that a traveling wave becomes elongated

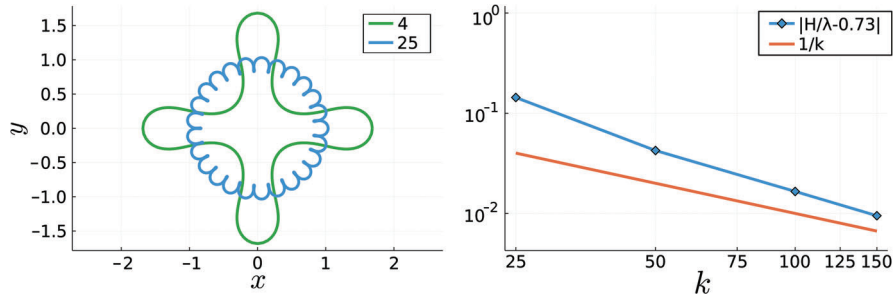

FIGURE 1 (Left panel) The shape of a perturbed droplet with $k = 4$ and $k = 25$. As the number of lobes k grows, the solution appears to converge to the Crapper wave,[12] and approaches a profile similar to the limiting wave with self-intersecting profile. However, when the number of lobes is small, the limiting scenario remains unclear. (Right panel): Wave steepness H/λ of self-intersecting solution approaches the value 0.73 associated with the limiting Crapper wave.

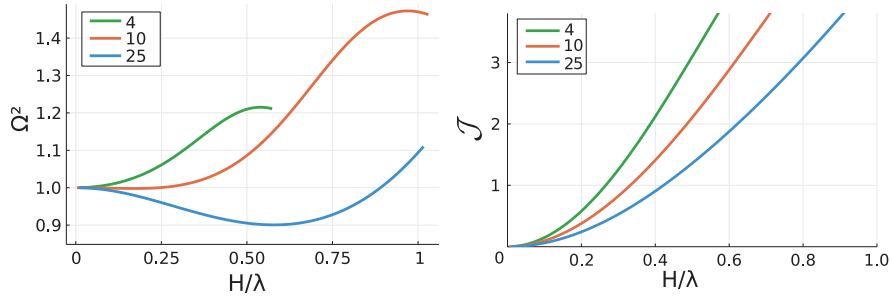

FIGURE 2 The left panel shows the square of the rotation speed Ω^2 as a function of steepness H/λ, and the right panel shows the angular momentum, $\mathcal{J}$, as a function of steepness H/λ.

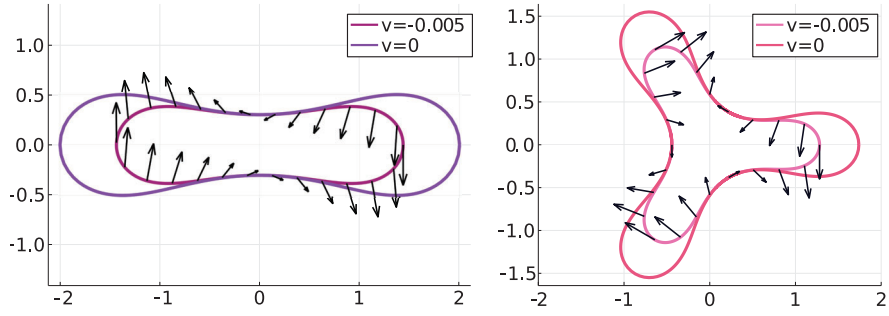

FIGURE 3 (Left panel) shows a two-lobed ($k = 2$) solution with $H/\lambda \approx 0.54$, and the (right panel) shows a three-lobed ($k = 3$) solution with $H/\lambda \approx 0.62$. The droplet shape is marked by dark violet line (left) and orange line (right), and the light violet (left) and pink (right) lines corresponds to a curve inside the fluid at $v = -0.005$. The velocity field is represented by black arrows.

as the steepness grows, and the number of Fourier modes necessary to resolve the solution grows with wave steepness (see Figure 4), indicating the existence of a singularity in the analytic continuation of $z(w)$ to the upper half-plane $w \in \mathbb{C}^+$. The nature of this singularity and the existence of a limiting wave are the subject of ongoing research.

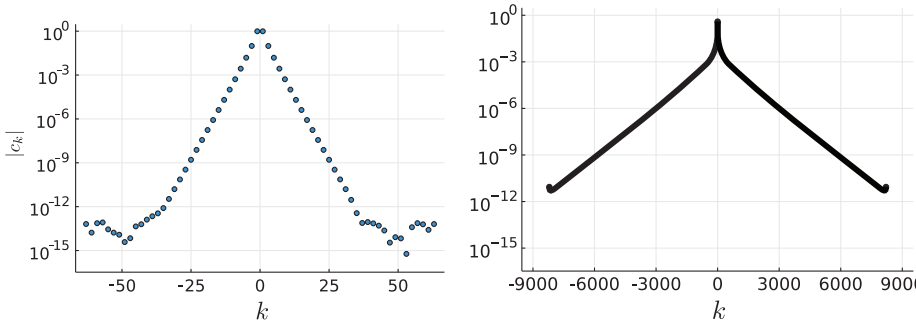

FIGURE 4 The Fourier spectrum for two nonlinear waves with two lobes ($k = 2$): (Left panel) shows the magnitude of Fourier coefficients for a wave with $H/\lambda \approx 0.06$, and (right panel) corresponds to $H/\lambda \approx 0.54$.

The numerical simulations and theoretical considerations suggest that a solution with sufficiently many lobes approaches the Crapper wave as the number of lobes grows (Figure 1). The right panel of Figure 1 indicates that steepness of the self-touching (limiting) Crapper wave is approached by the nonlinear solutions of (10) as the number of lobes k increases. This can be explained as follows: the wavelength is given by $\lambda = 2\pi/k$, and as it becomes small compared to the perimeter of the droplet (when k grows), the effects of local curvature become less significant and vanish in the limit $k \to \infty$. Another open question concerns the number of lobes for which self-touching of neighboring waves occurs (Crapper scenario) versus the presently unknown limiting scenario for few lobes, for example, $k = 2$ and $k = 3$ for which no indication of a tendency to self-intersect was observed.

7 | CONCLUSION

Breaking of water waves in deep ocean is associated with generation of water droplet spray. The latter partially accounts for the energy–momentum transfer in wave turbulence. The physical processes that generate water spray have been observed in ocean,[17] as well as theoretically.[18] As plunging breaker develops on the crest of an ocean wave, there is an abrupt growth of small scale features, and several physical mechanisms suddenly come into play.[19] The force of the surface tension, normally having little effect on long gravity waves, becomes one of the dominant forces at the crest of a breaking wave. The detachment of a water droplet from a plunging breaker is a complicated and nonlinear process, and the present work does not make an attempt to understand it to the full extent.

We considered a problem of deformation of a fluid disc with a free boundary subject to the force of surface tension. We found that a conformal map associated with such a flow satisfies a pseudodifferential equation that is similar to Babenko equation for the Stokes wave. We demonstrate the results of numerical simulation with initial data close to linear waves, and observe excellent agreement for small amplitude waves, and report significant deviations as amplitude grows.

The nonlinear equation (9), or its complex form (10), are solved by the Newton CR method[10,11] that is also applicable to the Stokes wave problem. The present work is a precursor to further investigation of nonlinear waves, and of particular interest are the questions of existence of the limiting wave, its nature, and singularities. One may speculate that the limiting wave will not form an angle on the surface, because it would make the potential energy grow; yet, the

numerical simulations suggest the breaking of a droplet (for small number of lobes), and a tendency to develop a self-touching solution like the Crapper wave (for large number of lobes). The study of limiting scenarios is the subject of ongoing work.

DATA AVAILABILITY STATEMENT

Data sharing not applicable to this article as no datasets were generated or analyzed during the current study.

ORCID

Alexander Chernyavsky https://orcid.org/0000-0002-3554-4599
Sergey Dyachenko https://orcid.org/0000-0003-1265-4055

REFERENCES

1. Longuet-Higgins M. The generation of capillary waves by steep gravity waves. *J Fluid Mech*. 1963;16:138-159.
2. Dyachenko AI, Korotkevich AO, Zakharov VE. Weak turbulent Kolmogorov spectrum for surface gravity waves. *Phys Rev Lett*. 2004;92:134501.
3. Korotkevich AO. Simultaneous numerical simulation of direct and inverse cascades in wave turbulence. *Phys Rev Lett*. 2008;101:074504.
4. Stokes G. On the theory of oscillatory waves. *Trans Camb Phil Soc*. 1847;8:411-455.
5. Ovsyannikov L. Dynamika Sploshnoi Sredy, Lavrentiev Institute of hydrodynamics. *Sib Branch Acad Sci USSR*. 1973;15:104.
6. Tanveer S. Singularities in water waves and Rayleigh–Taylor instability. *Proc R Soc London Ser A: Math Phys Sci*. 1991;435:137-158.
7. Crowdy D. Circulation-induced shape deformations of drops and bubbles: exact two-dimensional models. *Phys Fluids*. 1999;11:2836-2845.
8. Dyachenko SA. Traveling capillary waves on the boundary of a fluid disc. *Stud Appl Math*. 2022;148:125-140.
9. Babenko KI. Some remarks on the theory of surface waves of finite amplitude. In: *Doklady Akademii Nauk*. Vol 294. Russian Academy of Sciences; 1987:1033-1037.
10. Saad Y. *Iterative Methods for Sparse Linear Systems*. SIAM; 2003.
11. Yang J. Newton-conjugate-gradient methods for solitary wave computations. *J Comput Phys*. 2009;228:7007-7024.
12. Crapper G. An exact solution for progressive capillary waves of arbitrary amplitude. *J Fluid Mech*. 1957;2:532-540.
13. Longuet-Higgins M. Limiting forms for capillary-gravity waves. *J Fluid Mech*. 1988;194:351-375.
14. Rayleigh L. On the capillary phenomena of jets. *Proc R Soc London*. 1879;29:71-97.
15. Trinh E, Wang T. Large-amplitude free and driven drop-shape oscillations: experimental observations. *J Fluid Mech*. 1982;122:315-338.
16. Boyd JP. *Chebyshev and Fourier Spectral Methods*. Courier Corporation; 2001.
17. Erinin M, Wang S, Liu R, Towle D, Liu X, Duncan J. Spray generation by a plunging breaker. *Geophys Res Lett*. 2019;46:8244-8251.
18. Dyachenko S, Newell A. Whitecapping. *Stud Appl Math*. 2016;137:199-213.
19. Duncan JH, Qiao H, Philomin V, Wenz A. Gentle spilling breakers: crest profile evolution. *J Fluid Mech*. 1999;379:191-222.

How to cite this article: Chernyavsky A, Dyachenko S. Dynamics of 2D fluid in bounded domain via conformal variables. *Stud Appl Math*. 2023;1-10. https://doi.org/10.1111/sapm.12663